3 Molecular Crystal Project

Project Leader: Reiji Kumai

In this project, electronic correlation in molecular crystal systems is being investigated to elucidate novel phenomena such as superconductivity and charge ordering. We will analyze crystal structures of molecular crystals under high pressure and/or at low temperature to elucidate the origins of phase transitions.

3-1 Electronic ferroelectricity in a molecular crystal with large polarization directing antiparallel to ionic displacement

Switchable large polarization of ferroelectrics has opened the way to electronics applications such as capacitors, sensors, and data storage, as well as to electromechanical and optical devices. Whereas the sum of permanent dipole moments of polar ions determines the polarization of orientational "order-disorder-type" ferroelectrics, the product of relative displacement and charge of the ions had been the classical picture of polarization for "displacive-type" ferroelectrics. In actual ferroelectrics, however, even accurate knowledge of spatial charge distributions, which can be obtained in principle by precise X-ray structural analysis, cannot explain the macroscopic polarization quantitatively. The electric polarization can be correctly represented on the basis of quantum mechanical theory using the formalism of Berry phase by calculating the displacement current under changes of the electronic wave functions. This fact is especially important for the displacive-type ferroelectrics having some orbital hybridization between ions.

Here we address the extreme case in which the electronic process mostly governs the large polarization of a ferroelectric. The compound considered here is an organic charge-transfer complex of electron donor (*D*), tetrathiafulvalene (TTF) and acceptor (*A*), *p*-chloranil (CA) (Fig. 1) [1]. The key characteristic of this compound is a valence instability called the neutral-to-ionic transition (NIT), which arises from the delicate balance between the electrostatic energy gain and the energy cost of molecular ionization. According to the C=O stretch mode vibration frequency in the infrared spectra, averaged molecular ionicity was found to jump from ~0.3 for the quasi-neutral phase to ~0.6 for the quasi-ionic phase upon the NIT [2, 3].

The TTF-CA crystal comprises *DA* alternating stacks along the *a*-axis and the one-dimensional nature along this chain brings about the structural instability of Peierls or spin-Peierls type, displacing pairwise the ionized *D* and *A* molecules (Fig. 1(d)). Ferroelectricity emerges if the chain can invert its polarity as ..*DA* *DA* .. ↔ .. *AD* *AD*... where the underlines represent the dimerized *DA* pairs. The crystal structure is symmetry-broken to a polar space group of *Pn* upon NIT as determined by neutron and high-resolution X-ray diffraction experiments.

The TTF-CA complex can be regarded as a displacive-type ferroelectric because the molecules remain flat and nearly symmetric in shape; the dipole moments of both TTF and CA are negligibly small (< 0.1 Debye). The molecular charge $Ze = \pm 0.60(3)e$ and relative displacement (**u**) yield a dipole moment of $\mu^{(cell)} = \Sigma_{(cell)} Ze\mathbf{u} =$ [0.62(3), 0, 0.20(3)] Debye per unit cell (volume $V_{cell} = 779.02(13)$ Å^3), which corresponds to the small ionic polarization of $\boldsymbol{P}^{ion} = \mu^{(cell)}/V_{cell} =$ [0.27(2), 0, 0.09(2)] μCcm^{-2} at $T = 15$ K. In contrast to this conventional point-charge picture, the recent first-principles calculations invoked a much larger spontaneous polarization (3~10 μCcm^{-2} along the *a*-direction) with two contrasting candidates of electronic states [4, 5]; the total polarization is predicted to direct either parallel or antiparallel to the ion polarization, depending on the antiferromagnetic or nonmagnetic state, namely, the presence or absence of the $S = 1/2$ spins on each ionized molecule. Such predictions strongly motivated us to experimentally determine both the magnitude and the direction of spontaneous polarization.

The large ε_r is suggestive of a large spontaneous polarization as a proper ferroelectric. Nevertheless, its narrow charge gap of TTF-CA (~0.7 eV) gives rise to
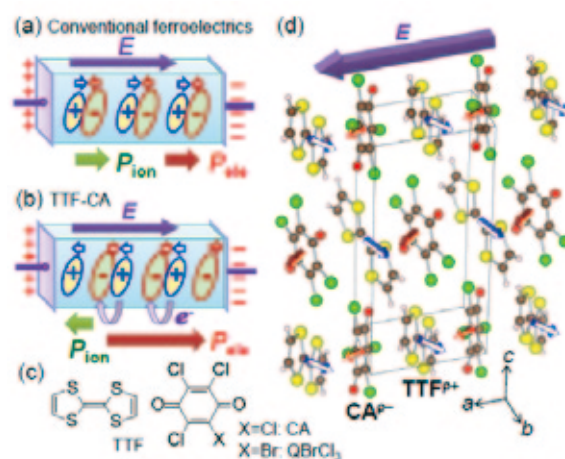

Fig. 1 Schematic illustrations of the electric polarization (solid arrows) and displacement direction (small open arrows) of ions in the conventional displacive-type ferroelectrics (a) and the TTF-CA crystal (b). (c) Molecular structures of TTF, CA, and QBrCl$_3$. (d) Crystal structure of TTF-CA and molecular displacement directions under electric field.

an incompletely-insulating electric resistivity as low as $\sim 10^{-8}$ Ωcm^{-1} even at low temperatures of around T_c and has long hindered the experimental evaluation of the spontaneous polarization value. Additional electric leakage under a higher field comes from the nonlinear electric transport and the current-induced resistance switching to a low-resistance state when the external electric field exceeds approximately 10 kVcm^{-1}. For this reason, the maximum field was kept below this value in the polarization hysteresis measurements, and satisfactory observations required further cooling. As exemplified by the 51 K data in Fig. 2, the rectangular P-E curvature at high frequencies well proves the ferroelectricity, although it becomes longitudinally warped due to electric leakage as the frequency decreases to 10 Hz. On the other hand, the coercive field E_c increases with increasing frequency or lowering temperature probably due to the rate-limiting domain-wall dynamics. Satisfactory observations of hysteresis were thereby limited in a narrow range of both frequency and temperature.
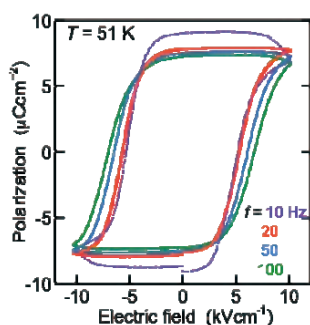

Fig. 2 The polarization measured with triangular ac electric field ($E||a$).

The symmetry-breaking of TTF-CA crystal structure under an electric field was probed by the difference in intensity between the Bijvoet pair (hkl versus $\bar{h}\bar{k}\bar{l}$) reflections, which arises from the anomalous X-ray scattering effect. The simulation based on the crystal structures at $T = 15$ and 40 K predicts that the Bijvoet pair reflections 101 and $\bar{1}0\bar{1}$ have sufficient intensities and are the most susceptible to the anomalous X-ray scattering for X-ray wavelength $\lambda = 1.55$ Å used. Figure 3(a) depicts the temperature dependence of their normalized integrated intensity $I_+ \equiv I(101)/\{I(101) + I(\bar{1}0\bar{1})\}$ and $I_- \equiv I(\bar{1}0\bar{1})/\{I(101) + I(\bar{1}0\bar{1})\}$. The crystal was cooled under a poling electric field of +4 kVcm^{-1} applied along the crystal a-direction. Note that the applied field is defined as plus when directed in the crystal a-direction. For temperatures above $T_c = 81$ K, this reflection intensity obeys Friedel's law $I_+ = I_- = 0.5$ expected for the centric (paraelectric) structure free from the anomalous X-ray scattering. Below T_c, one of

the I_+ and I_- decreases from 0.5 and the other increases, indicating breaking of symmetry with strong first-order nature. The I_+ and I_- of the Bijvoet pair were interchanged by inverting the electric field direction due to polarization switching, as exhibited for $T = 61$ K in Fig. 3(b). Just below T_c, the observed I_+ and I_- approach 0.705 or 0.295 (horizontal dotted lines in Fig. 3(a)), which corresponds to the full polarization into either polarity according to the simulation. Therefore, the poling field of 4 kVcm^{-1} is sufficient for developing a single-domain state.
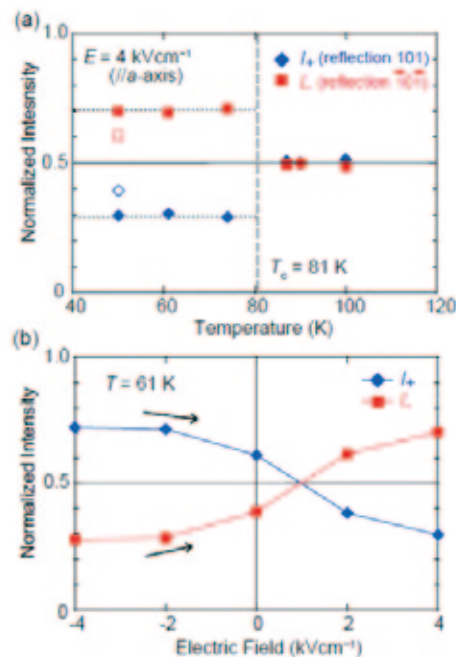

Fig. 3 Degree of bulk polarization under electric field E ($||a$) probed by the anomalous x-ray scattering effect. (a) Temperature dependence of normalized integrated intensity of Bijvoet pair reflections at constant $E = +4$ kVcm^{-1}. Open symbols are intensity data measured at 32 min after switching off to $E = 0$ at $T = 50$ K and represent a polarization decay toward the multi-domain state. (b) Normalized intensity under E increasing from -4 kVcm^{-1} to +4 kVcm^{-1} at 61 K.

By comparing the observed intensity of the Bijvoet pair (I_+ and I_-) with the simulation, we identified the absolute configuration of the crystal structure relative to the externally applied field. The positively charged TTF molecules shift toward the positive electrode and the negatively charged CA toward the negative electrode. The configuration with all the ionic charges displacing against the electric field is counterintuitive for the displacive-type ferroelectrics. Considering that the strong electric field always compels the total spontaneous polarization P_s to align in the same direction, P_s should direct antiparallel to the ionic

displacement. This picture is in accordance with the theoretical prediction assuming the nonmagnetic state rather than the antiferromagnetic state [4, 5].

At the earliest stage of research, the NIT was described by an electrostatic picture of Madelung energy gain vs. ionization energy of molecules. In contrast, the classical point-charge picture completely fails to explain both the magnitude and polarity of polarization. What is the origin of this large discrepancy? Judging from negligible molecular dipole moments and tiny ionic polarizations herein, a major contribution to the spontaneous polarization should be the electronic polarization. In the displacive-type ferroelectric oxides, Born effective charge Z^*, which relates the change of polarization $\Delta\mathbf{P}$ with displacement $\mathbf{u}$ as $\Delta\mathbf{P} = Z^*e\mathbf{u}/V_{cell}$, is enhanced by strong orbital hybridization, as compared to the formal valence state of ions. For instance, in $PbTiO_3$, first-principles calculations revealed $Z^*(Ti^{4+}) = +7.06$ and $Z^*(O^{2-}) = -5.83$ or -2.56 for $\mathbf{u}||<100>$. The TTF-CA system appears to be an extreme case exhibiting a colossal Z^* of opposite sign in comparison with the respective molecular valence (± 0.60); $Z^*(D) = -13.9$ and $Z^*(A) = +13.9$ were roughly estimated from relative displacement $u_x = 0.110$ Å and observed polarization $P_x = 6.3$ μCcm^{-2} through $P_x = 2Z^*eu_x/V_{cell}$. Actually, the highest occupied molecular orbital (HOMO) of TTF strongly hybridized with the lowest unoccupied one (LUMO) of CA, as evidenced by the large electron transfer interaction t (~0.24 eV) deduced by optical spectra.

In conclusion, the colossal effective Born charges of opposite signs of the constituent ions strongly indicate the genuine "electronic ferroelectricity" in the nominally ionic molecular compound TTF-CA. Such an electronic process governs the magnitude and even the direction of macroscopic polarization. The electronic ferroelectricity itself is an emerging phenomenon in the correlated electron system, such as charge-ordered ferroelectrics and spin-driven ferroelectrics called multiferroics [6]. The electronic response with less energetic cost of lattice deformations in the present molecular system promises both high-performance and high-frequency operations as well as new functionalities. For highly-functional ferroelectricity in molecular systems, we consider that substantial covalency between interacting molecular orbitals may be the key to overcoming the small ionic charge, dilute dipole density inherent to molecular crystals, and even the least permanent molecular dipoles.

[1] J. B. Torrance *et al.*, *Phys. Rev. Lett.*, **46**, 253 (1981).
[2] A. Girlando *et al.*, *J. Chem. Phys.* **79**, 1075 (1983).
[3] S. Horiuchi *et al.*, *J. Phys. Soc. Jpn.*, **69**, 1302 (2000).
[4] G. Giovannetti *et al.*, *Phys. Rev. Lett.*, **103**, 266401 (2009).
[5] S. Ishibashi *et al.*, *Physica B*, **405**, S338 (2010).
[6] S. Ishihara, *J. Phys. Soc. Jpn.*, **79**, 011010 (2010).

3-2 X-ray structural study of an electric-field-induced state in the charge ordered organic salt β-(BEDT-TTF)$_2$PF$_6$

There have been several recent studies on nonlinear properties in organic conductors. In particular, the responses of nonlinear conduction under an external electric field and electric-field-induced metastable states have attracted much attention because of their applications in engineering and theory.

The charge ordered organic salt β-(BEDT-TTF)$_2$PF$_6$ exhibits nonlinear conduction at low temperatures. This salt undergoes metal–insulator transition at 297 K, below which the superlattice reflections corresponding to (a, b, $2c$) were observed [1, 2].
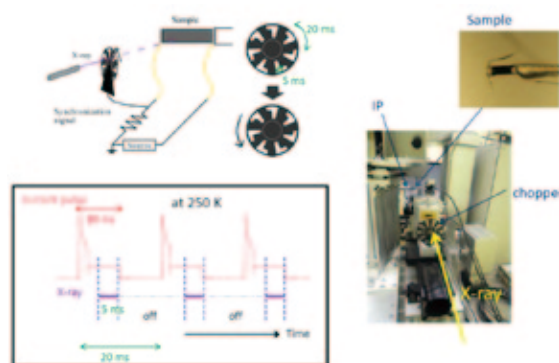

Fig. 1 X-ray diffraction synchronized with the nonlinear conduction.

In the current–voltage characteristics, the negative differential resistance (NDR) is observed at 290 K and the giant nonlinearity accompanied by NDR appears below 272 K. This salt in the NDR region arises from the high resistance state to the low resistance state for about 5 ms by applying a pulse of current with a pulse width of 10 ms. Time-resolved experiments using X-ray diffraction were performed at BL-8A. This condition appears repeatedly while the recovery period of the sample condition is 10 ms. The X-ray beam was synchronized with the sample condition as shown in Fig. 1. We attempted to perform diffraction measurements in the low resistance state.

Figure 2(a) shows oscillation photographs at the external current of 0 mA (upper) and the external current of 0.9 mA (lower). The peak splitting and the broadening of fundamental and superlattice reflections were not observed in the electric field, indicating that the phase coexistence of the charge ordering state and

the other state did not occur. The intensities of superlattice reflections in an electric field were decreased by an average of 30%, although the intensities of fundamental reflections were almost the same (see Fig. 2(b)). The volume of the unit cell was increased by 0.43%. This value was smaller than that estimated from the temperature dependence of the superlattice intensities. This suggested that the phenomenon of charge-order melting is an intrinsic electric field-induced effect and is not only related to the Joule heating effect. In a future work, we will try to determine the structure using time-resolved experiments to elucidate the electric field-induced melting of charge-order.

[1] T. Mori *et al.*, *Solid State Comm.*, **53**, 627 (1985).
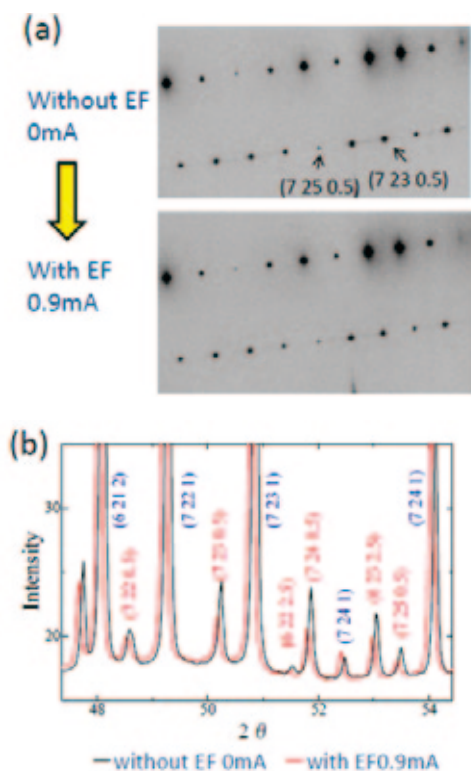[2] G. K. Rohan *et al.*, *J. Phys. Soc. Jpn*, **67**, 4193 (1998).

Fig. 2 (a) Oscillation photograph by X-ray diffraction in an electric field at 240 K. (b) XRD profiles at external currents of 0 mA and 0.9mA are indicated by black and red lines, respectively.

3-3 Structural study of charge ordered insulating state in DODHT salts

The relationship between charge ordering and superconductivity is of interest in strongly correlated electron materials in association with the charge fluctuation and the emergence of superconductivity. New radical salts based on an organic donor, DODHT, which tends to give strongly correlated electron systems due to its reduced -electron system as compared with the conventional TTF donors, were synthesized with the aim of developing superconductors [1]. Several superconductors under pressure have been found to date. All the superconducting salts are crystallized in the β"-type donor arrangement, and the consequent band structure is quarter-filling and the Fermi surface consists of one quasi-one-dimensional open and one quasi-two-dimensional closed Fermi surface. Charge ordering and superconductivity coexist in a pressure-temperature phase diagram observed by detailed transport measurements. Previous X-ray diffraction studies clarified the crystal structure with the stripe-type charge order pattern where the electron-rich site and the electron-poor site were arranged alternately along the a axis in the PF_6 salt. This result was consistent with magnetic behavior as the 1D alternating Heisenberg chain model [2]. On the other hand, the AsF_6 salt exhibits an abrupt drop in the magnetic susceptibility at 90 K (see Fig. 1(a)). The temperature dependence of the magnetic susceptibility above 90 K is also slightly different from that of the PF_6 salt. The degree of the charge disproportionation or charge pattern of AsF_6 salt may be different. We performed an X-ray diffraction study to investigate the crystal structure of the AsF_6 salt.

The structural change at low temperature was examined from oscillation photographs. Superstructure reflections with diffuse streaks along the b^* direction, indicated by arrows in Fig. 1(b), were observed below about 200 K. The diffuse reflections below 45 K correspond to $q = (a^*/2, b^*/2, c^*)$ indicating the $(a+b)$ x $(a-b)$ x c unit cell. The doubled period along the diagonal direction is expected to be due to the stripe-type arrangement along the a axis, where a is the lattice parameter at room temperature, as shown in Fig. 2. This charge order pattern is different from that of the PF_6 salt. We also searched for structural anomalies above 90 K with decreasing temperature. Crystal structure analysis and band structure calculations at 250 K and 150 K were carried out on the basis of the fundamental structure. The shape of Fermi surfaces at 150 K became one-dimensional compared to that at 250 K, indicating nesting below 90 K.
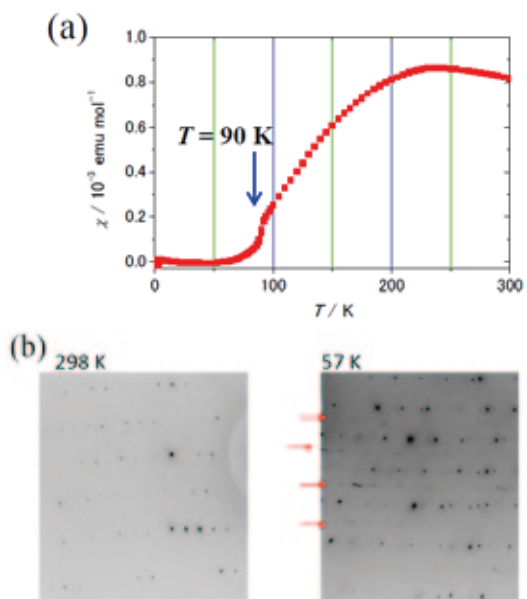
Fig. 1 (a) Temperature dependence of the magnetic susceptibility for the AsF_6 salt. (b) Oscillation photographs measured by synchrotron X-ray diffraction at 298 K and 57 K.
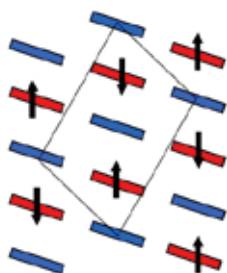

Fig. 2 Schematic illustration of the crystal structure with the stripe-type arrangement for charge ordering phase in AsF_6 salt.

[1] H. Nishikawa *et al.*, *J. Am. Chem. Soc.*, **124** (2002) 730.
[2] H. Nishikawa *et al.*, *Phys. Rev. B*, **72**, 2005, 052510.